International Journal of Numerical Methods for Heat & Fluid Flow

Effects of hall and ion slip on MHD peristaltic flow of Jeffrey fluid in a non-uniform rectangular duct

R. Ellahi M. M. Bhatti Ioan Pop

Effects of hall and ion slip on MHD peristaltic flow of Jeffrey fluid in a non-uniform rectangular duct

Received 2 February 2015
Revised 6 July 2015
Accepted 13 July 2015

R. Ellahi
Department of Mathematics and Statistics, FBAS, IIUI, Islamabad, Pakistan and Department of Mechanical Engineering, University of California Riverside, Riverside, California, USA
M.M. Bhatti
Shanghai Institute of Applied Mathematics and Mechanics, Shanghai University, Shanghai, China, and
Ioan Pop
Department of Mathematics, Babeş-Bolyai University, Cluj-Napoca, Romania and Department of Mathematics, University of Cluj, Cluj-Napoca, Romania

Abstract
Purpose – The purpose of this paper is to theoretically study the problem of the peristaltic flow of Jeffrey fluid in a non-uniform rectangular duct under the effects of Hall and ion slip. An incompressible and magnetohydrodynamics fluid is also taken into account. The governing equations are modelled under the constraints of low Reynolds number and long wave length. Recent development in biomedical engineering has enabled the use of the periastic flow in modern drug delivery systems with great utility.
Design/methodology/approach – Numerical integration is used to analyse the novel features of volumetric flow rate, average volume flow rate, instantaneous flux and the pressure gradient. The impact of physical parameters is depicted with the help of graphs. The trapping phenomenon is presented through stream lines.
Findings – The results of Newtonian fluid model can be obtained by taking out the effects of Jeffrey parameter from this model. No-slip case is a special case of the present work. The results obtained for the flow of Jeffrey fluid reveal many interesting behaviours that warrant further study on the non-Newtonian fluid phenomena, especially the shear-thinning phenomena. Shear-thinning reduces the wall shear stress.
Originality/value – The results of this paper are new and original.
Keywords MHD, Rectangular duct, Peristaltic flow, Hall effect, Ion slip, Jeffrey fluid
Paper type Research paper

Nomenclature

S	stress tensor	M	MHD parameter
P	pressure	X	direction of wave propagation
X	wave propagation	Q	flow rate
c	velocity of the propagation	j	current density

International Journal of Numerical Methods for Heat & Fluid Flow
Vol. 26 No. 6, 2016
pp. 1802-1820

0961-5539
DOI 10.1108/HFF-02-2015-0045

R. Ellahi is grateful to Pakistan Council for Science and Technology (PCST) to honour him with 7th top most Productive Scientist of Pakistan Award "Category A".

Greek symbols

λ	wavelength
ρ	density
μ	dynamic viscosity
ϕ	amplitude ration
β	aspect ratio
λ_1	Jeffrey parameter
$\dot{\gamma}$	shear rate
ψ	stream function
δ	wave length
σ	conductivity of the fluid
ω_e	cyclotron frequency
τ_e	electron collision time
β_i	ion-slip parameter
β_e	hall parameter

1. Introduction

The Newtonian and non-Newtonian fluids have received great attention for the last three decades because of their application in pharmaceuticals, physiology, fibre technology, food products, coating of wires, crystal growth, certain paints, salt solutions, molten polymers, ketchup, custard, toothpaste, starch suspensions, paints, blood at low shear rate and shampoo are few examples of the non-Newtonian fluids. Such fluids in view of diverse characteristics cannot be examined by using single constitutive relationship. These fluids have been classified into three types, namely, differential, rate and integral, etc. (Rajagopal, 1978, 1982, 1983; Rajagopal and Gupta, 1984; Ellahi, 2010, 2013; Fetecau and Fetecau, 2005, 2006). Characteristics of non-Newtonian fluids cannot be described by a single constitutive relationship. Hence various models of non-Newtonian fluids have been proposed. Usually the non-Newtonian fluids are divided into three types, i.e., rate type, differential type and integral type. Rate type fluids describe the behaviour of relaxation and retardation times. Maxwell fluid is a simplest subclass of rate type material which exhibits the behaviour of relaxation time only. This model does not present the behaviour of retardation time. Consequently the Jeffrey fluid model is proposed to fill this void. Moreover, the biofluids in physiological system have also been investigated to find the treatment of diagnostic problems that arise during circulation in a human body. There are several models which have been proposed to describe such physiological fluids, however, their full potential has not been exploited yet and a lot of questions remain unresolved. It is also speculated that the physiological fluids such as blood exhibit Newtonian and non-Newtonian behaviours at once. Among said models, non-Newtonian Jeffrey model is significant for polymer industries and biofluids simultaneously. It is also worth mentioning that Newtonian fluid model can be deduced from Jeffrey model as a special case by taking $\lambda_1 \to 0$. A Jeffery fluid model has been selected here, because it has a different rheology than a viscous fluid (Kothandapani and Srinivas, 2008; Hayat *et al.*, 2011).

Furthermore, the phenomenon of peristaltic transport has enjoyed increased interest from investigators in different disciplines. Basically peristaltic word comes from Greek word peristaltikos which means compressing and clasping. Peristaltic wave is generated when progressive area of contraction or expansion propagates along the length of distensible tube containing fluid. Some typical applications of these kinds of flow problems are transport of spermatozoa in the ducts efferent of the male reproductive tract, urine transport from kidney to bladder, transport of lymph in the lymphatic vessels, vasomotor of small blood vessels such as arterioles, venues and capillaries movement of ovum in the female fallopian tube, movement of chyme in the gastrointestinal tract. The mechanism of peristaltic transport has also been exploited for industrial applications like, sanitary fluids, transport of noxious fluid in nuclear industry, transport of corrosive fluids where the contact of the fluid with the machinery parts is prohibited and blood transport in heart lung machine, etc. Several theoretical and experimental investigations have been made with different fluids in different geometries to understand the peristaltic motion. Some relevant studies in various situations can be seen from the list of references (Mekheimer, 2003; Akbar and Nadeem, 2011; Safia *et al.*, 2012; Ellahi *et al.*, 2013, 2016a) and several therein.

The discipline of slip effects may appear for two types of fluids, namely, rare field gases (Chu and Fang, 2000) and fluids having much more elastic character. In these fluids, slippage appears subject to large tangential traction. It is noticed through experimental and theoretical observations (Vinogradov and Ivanova, 1968; Luk *et al.*, 1987; Ellahi *et al.*, 2016b; White *et al.*, 1991; Hatzikiriakos and Dealy, 1992; Migler *et al.*, 1993; Piau and El Kissi, 1994) that the occurrence of slippage is possible in the non-Newtonian fluids, molten polymer and polymer solution. In addition, a clear layer is sometimes found next to the wall when flow of dilute suspension of particles examined. In experimental physiology such a layer is observed when blood flow through capillary vessels is studied by Coleman *et al.* (1996). The fluids that exhibit slip effect have many applications, for instance, the polishing of artificial heart valves and internal cavities (Roux, 1999). In all these studies the peristaltic flow problems have been extensively investigated with no-slip condition. Very less emphasis has been given to such flows in the presence of a slip condition. Although, the application of slip condition in the peristaltic flows has special relevance in physiology and polymers. The effects of slip conditions have discussed by Ebaid (2008), and Taneja and Jain (2004).

It is well known that in an ionized gas when the strength of the magnetic field is very strong, one cannot neglect the Hall effects. Attia (2004) had examined unsteady Hartmann flow with heat transfer of a viscoelastic fluid taking the Hall Effect into account. Abo-Eldahab *et al.* (2010a, b) investigated the effects of Hall and ion-slip currents on magnetohydrodynamic (MHD) peristaltic transport and couple stress fluid. Rathod and Mahadev (2012) studied the peristaltic flow of Jeffrey fluid with slip effects in an inclined channel. Gad (2010) presented the effect of Hall current on interaction of pulsatile and peristaltic transport induced flows of a particle – fluid suspension. Srinivasacharya and Kaladhar (2012) examined the analytical solution for Hall and ion-slip effects on mixed convection flow of couple stress fluid between parallel disks. Elgazery (2009) studied the effects of chemical reaction, Hall and ion-slip currents on MHD flow with temperature dependent viscosity and thermal diffusivity. In addition, MHD flow problems have attracted the attention scientist due to its applications such as magnetic wound or cancer tumour treatment causing magnetic hyperthermia, magnetic devices for cell separation, targeted transport of drugs using magnetic particles as drug carriers, reduction of bleeding during surgeries or provocation of occlusion of feeding vessels of cancer tumours and development of magnetic tracers, etc. (Hameed and Nadeem, 2007; Mansour *et al.*, 2000; Lajvardi *et al.*, 2010; Makinde and Onyejekwe, 2011; Akram and Nadeem, 2013; Ellahi, 2013).

It is noticed from the available literature that a very few amount of literature is present on peristaltic flow in rectangular duct. Subba Reddy *et al.* (2005) have examined the influence of lateral walls on peristaltic flow in a rectangular duct. Tsangaris and Vlachakis (2003) have also found the exact solution of the Navier-Stokes equations (Tan and Masuoka, 2005, 2007) for the fully developed, pulsating flow in a rectangular duct with a constant cross-sectional velocity. To the best of our knowledge, no attention has been accorded yet to discuss the effects of hall with Ion slip for the flow of non-Newtonian Jeffrey fluid in a non-uniform rectangular duct. In this investigation such analysis is presented for title problem. Mathematical results under the consideration of long wavelength and low Reynolds number approximations are first derived analytically and then analysed carefully. It is worth mentioning that the Jeffrey model can indicate the changes of rheology on peristaltic flow not only for long wavelength, low Reynolds number assumptions but also for small or large amplitude ratio. Numerical computations have been used to evaluate the expression for pressure rise. Finally, the effects of various emerging parameters are discussed through graphs. The stream lines and trapping phenomenon have also been presented. This paper is designed as follows: Section 2 presents the mathematical model wherein a dimensionless set of governing equations subject to appropriate boundary conditions is derived. Analytical solutions are developed in Section 3. The final section provides detailed computational results with discussion and physical interpretation of our findings.

2. Mathematical formulation of the problem

Let us consider the flow of an incompressible Jeffrey fluid through a porous medium under the effects of MHDs in a rectangular duct having the channel width $2d$ and height $2a+kx$. We are considering Cartesian coordinate system such that X-axis is taken along the axial direction, Y-axis is taken along the lateral direction and Z-axis is taken along the vertical direction of the rectangular duct (see Figure 1).

The peristaltic waves on the walls are described as:

$$Z = H(X, t) = \pm a \pm kx \pm b \sin\left[\frac{2\pi}{\lambda}(X - ct)\right] \tag{1}$$

where b is the amplitudes of the waves, λ the wavelength, c the velocity of the propagation, t the time and X the direction of wave propagation. The walls parallel to XZ plane are not distracted and are not subject to any peristaltic wave motion. Let $(U, 0, W)$ be the velocity for the flow in a rectangular duct. The generalized Ohm's law with hall and ion-slip effect can be written as:

$$j = \sigma(E + V \times B) - \frac{\omega_e \tau_e}{B_0}(j \times B) - \frac{\omega_e \tau_e \beta_i}{B_0^2}[(j \times B) \times B] \tag{2}$$

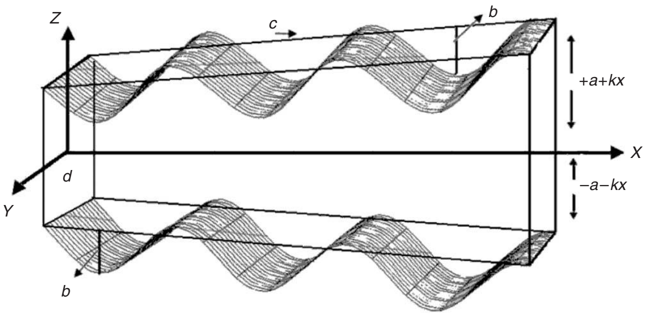

Figure 1. Geometry of the problem

where B, E, V, j, σ, ω_e, τ_e and β_i are the magnetics field vector, the electric field, the fluid velocity vector, the current density vector, the conductivity of the fluid, the cyclotron frequency, the electron collision time and the slip parameter. The Equation (2) can be written as:

$$\left(1+\beta_i\beta_e\right)j_x-\beta_e j_z = \sigma(E_x-B_0 w) \tag{3}$$

$$\left(1+\beta_i\beta_e\right)j_z+\beta_e j_x = \sigma(E_z+B_0 u) \tag{4}$$

where $\beta_e = \omega_e\tau_e$ is the hall parameter. Solving for j_x and j_z we get:

$$j_x = \frac{\sigma\left[\left(1+\beta_i\beta_e\right)(E_x-B_0 w)+\beta_e(E_z+B_0 u)\right]}{\left(1+\beta_i\beta_e\right)^2+\beta_e^2} \tag{5}$$

$$j_z = \frac{\sigma\left[\left(1+\beta_i\beta_e\right)(E_z+B_0 u)-\beta_e(E_x-B_0 w)\right]}{\left(1+\beta_i\beta_e\right)^2+\beta_e^2} \tag{6}$$

The continuity equations for the incompressible Jeffrey fluid are stated as:

$$\frac{\partial U}{\partial X}+\frac{\partial W}{\partial Z} = 0 \tag{7}$$

Using Equations (5) and (6) the equation of motion along X-, Y- and Z-direction are:

$$\rho\left(\frac{\partial U}{\partial t}+U\frac{\partial U}{\partial X}+W\frac{\partial U}{\partial Z}\right) = -\frac{\partial P}{\partial X}+\frac{\partial}{\partial X}S_{XX}+\frac{\partial}{\partial Y}S_{XY}+\frac{\partial}{\partial Z}S_{XZ}+j_x\times B \tag{8}$$

$$0 = -\frac{\partial P}{\partial Y}+\frac{\partial}{\partial X}S_{YX}+\frac{\partial}{\partial Y}S_{YY}+\frac{\partial}{\partial Z}S_{YZ} \tag{9}$$

$$\rho\left(\frac{\partial W}{\partial t}+U\frac{\partial W}{\partial X}+W\frac{\partial W}{\partial Z}\right) = -\frac{\partial P}{\partial Z}+\frac{\partial}{\partial X}S_{ZX}+\frac{\partial}{\partial Y}S_{ZY}+\frac{\partial}{\partial Z}S_{ZZ}+j_z\times B \tag{10}$$

in which ρ is the density, P the pressure and $\mathbf{S}$ the stress tensor for Jeffrey fluid, which is defined as:

$$\mathbf{S} = \frac{\mu}{1+\lambda_1}(\dot{\boldsymbol{\gamma}}+\lambda_2\ddot{\boldsymbol{\gamma}}) \tag{11}$$

In the above equation, λ_1 is the ratio of the relaxation to retardation times, λ_2 the delay time, $\dot{\gamma}$ the shear rate and dots denote the differentiation with respect to time. Let us define a wave frame (x, y) moving with the velocity c away from the fixed frame (X, Y) by the following transformation:

$$x = X-ct,\ y = Y,\ z = Z,\ u = U-c,\ w = W,\ p(x,z) = P(X,Z,t) \tag{12}$$

Introducing the following non-dimensional quantities:

$$\bar{x}=\frac{x}{\lambda},\ \bar{y}=\frac{y}{d},\ \bar{z}=\frac{z}{a},\ \bar{u}=\frac{u}{c},\ \bar{w}=\frac{w}{c\delta},\ \bar{t}=\frac{ct}{\lambda},\ \bar{h}=\frac{H}{a},\ \bar{p}=\frac{a^2p}{\mu c\lambda}$$

$$Re=\frac{\rho ac}{\mu},\ \delta=\frac{a}{\lambda},\ \phi=\frac{b}{a},\ \overline{S}_{\overline{xx}}=\frac{a}{\mu c}S_{xx},\ \overline{S}_{\overline{xy}}=\frac{d}{\mu c}S_{xy},\ M=\sqrt{\frac{\sigma}{\mu}}B_0a$$

$$\overline{S}_{\overline{xz}}=\frac{a}{\mu c}S_{xz},\ \overline{S}_{\overline{yz}}=\frac{d}{\mu c}S_{yz},\ \overline{S}_{\overline{zz}}=\frac{\lambda}{\mu c}S_{zz},\ \overline{S}_{\overline{yy}}=\frac{\lambda}{\mu c}S_{yy},\ \beta=\frac{a}{d}$$

$$\bar{\dot{\gamma}}=\frac{\dot{\gamma}d_1}{c},\ K^*=\frac{k}{a} \tag{13}$$

Using the above non-dimensional quantities in Equations (2)-(5) and neglecting the electric field, the resulting equations can be written as:

$$\frac{\partial u}{\partial x}+\frac{\partial w}{\partial z}=0, \tag{14}$$

$$Re\delta\left(u\frac{\partial u}{\partial x}+w\frac{\partial u}{\partial z}\right)=-\frac{\partial p}{\partial x}+\delta\frac{\partial}{\partial x}S_{xx}+\beta^2\frac{\partial}{\partial y}S_{xy}+\frac{\partial}{\partial z}S_{xz}-\frac{M^2\left[(1+\beta_i\beta_e)(u+1)-\beta_e(-\delta w)\right]}{(1+\beta_i\beta_e)^2+\beta_e^2} \tag{15}$$

$$0=\frac{\partial p}{\partial y}+\delta^2\frac{\partial}{\partial x}S_{yx}+\delta^2\frac{\partial}{\partial y}S_{yy}+\delta\frac{\partial}{\partial z}S_{yz}, \tag{16}$$

$$Re\delta^2\left(u\frac{\partial w}{\partial x}+w\frac{\partial w}{\partial z}\right)=-\frac{\partial p}{\partial z}+\delta^2\frac{\partial}{\partial x}S_{zx}+\delta\beta^2\frac{\partial}{\partial y}S_{zy}+\delta^2\frac{\partial}{\partial z}S_{zz}-\frac{\delta M^2\left[(1+\beta_i\beta_e)(-\delta w)+\beta_e(u+1)\right]}{(1+\beta_i\beta_e)^2+\beta_e^2} \tag{17}$$

where:

$$S_{xx}=\frac{2\delta}{1+\lambda_1}\left(1+\frac{\lambda_2c\delta}{a}\left(u\frac{\partial}{\partial x}+w\frac{\partial}{\partial x}\right)\right)\frac{\partial u}{\partial x} \tag{18}$$

$$S_{xy}=\frac{1}{1+\lambda_1}\left(1+\frac{\lambda_2c\delta}{a}\left(u\frac{\partial}{\partial x}+w\frac{\partial}{\partial x}\right)\right)\frac{\partial u}{\partial y} \tag{19}$$

$$S_{xz}=\frac{1}{1+\lambda_1}\left(1+\frac{\lambda_2c\delta}{a}\left(u\frac{\partial}{\partial x}+w\frac{\partial}{\partial x}\right)\right)\left(\frac{\partial u}{\partial z}+\delta^2\frac{\partial w}{\partial x}\right) \tag{20}$$

$$S_{yy}=0 \tag{21}$$

$$S_{yz} = \frac{\delta}{1+\lambda_1}\left(1+\frac{\lambda_2 c\delta}{a}\left(u\frac{\partial}{\partial x}+w\frac{\partial}{\partial x}\right)\right)\frac{\partial w}{\partial y} \tag{22}$$

$$S_{zz} = \frac{2}{1+\lambda_1}\left(1+\frac{\lambda_2 c\delta}{a}\left(u\frac{\partial}{\partial x}+w\frac{\partial}{\partial x}\right)\right)\frac{\partial w}{\partial z} \tag{23}$$

Under the assumption of long wave length $\delta \leqslant 1$ and low Reynolds number $Re \to 0$, Equations (15)-(23) takes the form:

$$\beta^2\frac{\partial^2 u}{\partial y^2}+\frac{\partial^2 u}{\partial z^2}+\frac{M^2\left[(1+\beta_i\beta_e)(1+\lambda_1)\right]u}{(1+\beta_i\beta_e)^2+\beta_e^2} = (1+\lambda_1)\frac{dp}{dx}+\frac{M^2\left[(1+\beta_i\beta_e)(1+\lambda_1)\right]}{(1+\beta_i\beta_e)^2+\beta_e^2} \tag{24}$$

The corresponding boundary conditions are:

$$u = -1 \text{ at } y = \pm 1 \tag{25}$$

$$u = -1 \ \ at \ \ z = \pm h(x) = \pm 1 \pm K^* x \pm \phi \sin 2\pi x \tag{26}$$

where $0 \leqslant \phi \leqslant 1$.

3. Solution of the problem

The exact solution of the above non-homogenous partial differential Equation (24) satisfying the boundary conditions (25) and (26) can be written as:

$$u(x,y,z) = \sum_{m=1}^{\infty}\left[\frac{A_m \cosh\zeta y}{\sec\sqrt{\lambda_m z}}+\left(\frac{C_1}{C_0}-1\right)\frac{\cos\sqrt{C_0 z}}{\cos\sqrt{C_0 h}}-\frac{C_1}{C_0}\right] \tag{27}$$

where:

$$A_m = \frac{(C_0-C_1)\left(-2C_0\frac{\sin\sqrt{\lambda_m h}}{\sqrt{\lambda_m}}+\frac{2\sqrt{C_0}}{\cot\sqrt{C_0}h\sec\sqrt{\lambda_m h}}\right)}{h(x)C_0(C_0+\lambda_m)\cos\zeta} \tag{28}$$

$$\lambda_m = \left(\frac{\alpha_m}{h}\right)^2,\ C_0 = \frac{M^2\left[(1+\beta_i\beta_e)(1+\lambda_1)\right]}{(1+\beta_i\beta_e)^2+\beta_e^2},\ \varsigma = \sqrt{\left(\frac{C_0+\lambda_m}{\beta^2}\right)} \tag{29}$$

$$C_1 = \frac{M^2\left[(1+\beta_i\beta_e)(1+\lambda_1)\right]}{(1+\beta_i\beta_e)^2+\beta_e^2}+(1+\lambda_1)\frac{dp}{dx},\ \alpha_m = \frac{(2m-1)\pi}{2} \tag{30}$$

The volumetric flow rate is given by:

$$q = \int_0^1\int_0^{h(x)} u(x,y,z)dydz \tag{31}$$

and the instantaneous flux is given by:

$$\overline{Q} = \int_0^1\int_0^{h(x)} (u+1)dydz = q+h(x) \tag{32}$$

The average volume flow rate over one period ($T = \lambda/c$) of the peristaltic wave is defined as:

$$Q = \frac{1}{T}\int_0^T \overline{Q}dt = q + 1 \tag{33}$$

The pressure gradient dp/dx is obtained after solving Equations (32) and (33). Numerical integration for the integral given in Equation (31) is performed using software built-in Mathematica.

4. Results and discussion

In this section, we will discuss the effect of various interesting parameters on velocity u and pressure gradient dp/dx. The trapping mechanism has also been taken into account. Figure 2-19 have been drawn to measure the features of all parameters.

4.1 Pumping characteristics

Figures 2-7 present the effect of different parameters on velocity. Figure 2 depicts that with the increase of volumetric flow rate Q the velocity field increases. From Figure 3, it can be easily noticed that near the walls of the channel the velocity is increasing when

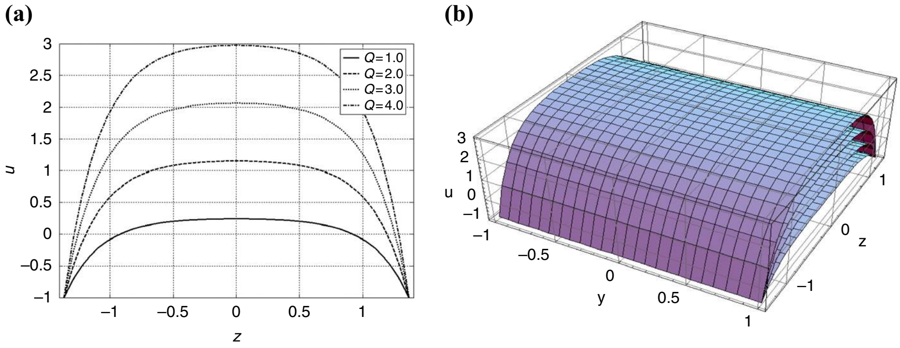

Notes: (a) For two-dimensional; (b) for three-dimensional

Figure 2. Velocity profile for different values of Q for fixed $M = 0.5$, $\beta_i = 0.93$, $\beta_e = 0.8$, $\beta = 0.5$, $\phi = 0.6$, $x = 0.1$, $\lambda_1 = 1$, $y = 0.4$, $K^* = 0.1$

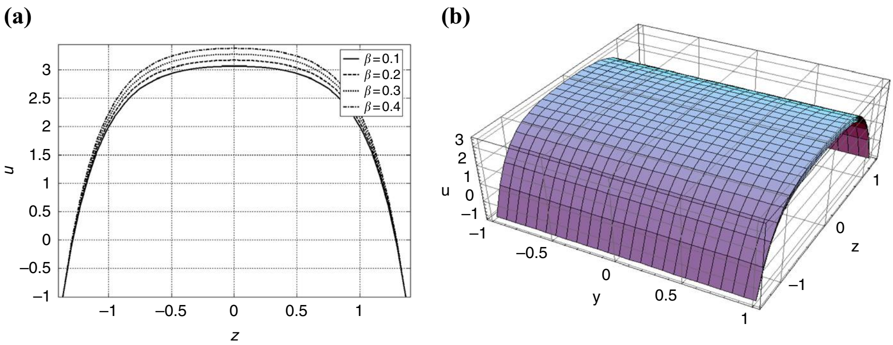

Notes: (a) For two-dimensional; (b) for three-dimensional

Figure 3. Velocity profile for different values of β for fixed $M = 0.5$, $\beta_i = 0.5$, $\beta_e = 0.8$, $Q = 4$, $\phi = 0.6$, $x = 0.1$, $\lambda_1 = 2$, $y = 0.4$, $K^* = 0.1$

the aspect ratio β increases while it decreases in the centre of the channel. It can be noticeable from Figure 4 that magnitude of the velocity is decreasing when the Hartmann number M increases, but near the walls, behaviour is opposite. Figure 5 illustrates that when the Jeffrey parameter λ_1 increases, the velocity field decreases.

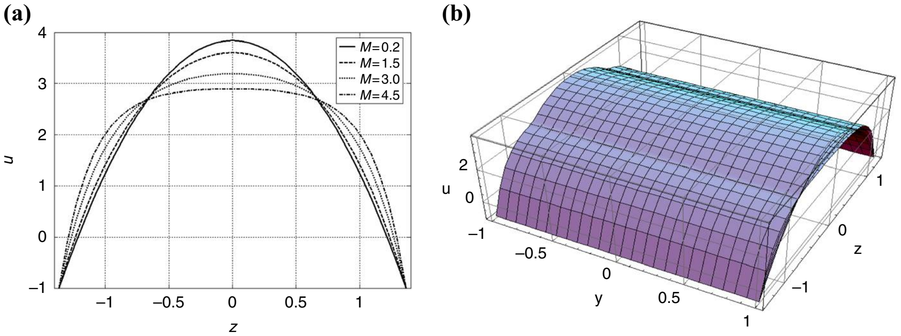

Notes: (a) For two-dimensional; (b) for three-dimensional

Figure 4.
Velocity profile for different values of M for fixed $\beta = 0.1$, $\beta_i = 0.95$, $\beta_e = 0.9$, $Q = 4$, $\phi = 0.6$, $x = 0.1$, $\lambda_1 = 0.1$, $y = 0.4$, $K^* = 0.1$

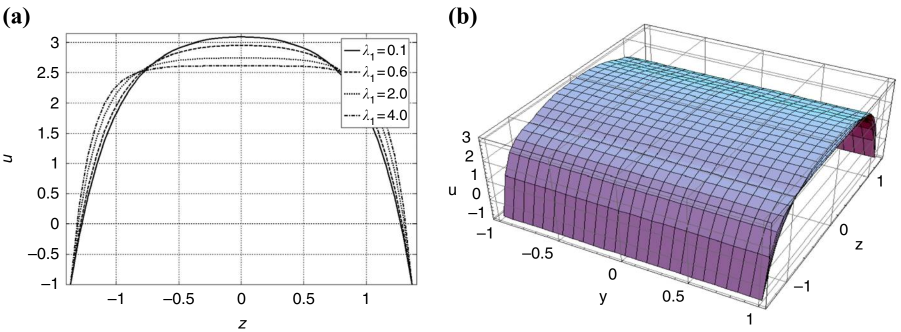

Notes: (a) For two-dimensional; (b) for three-dimensional

Figure 5.
Velocity profile for different values of λ_1 for fixed $\beta = 0.05$, $\beta_i = 0.99$, $\beta_e = 0.9$, $Q = 4$, $\phi = 0.6$, $x = 0.1$, $M = 2$, $y = 0.4$, $K^* = 0.1$

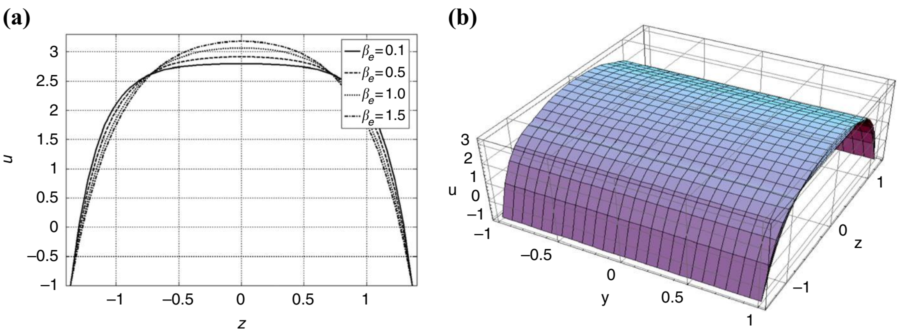

Notes: (a) For two-dimensional; (b) for three-dimensional

Figure 6.
Velocity profile for different values of β_e for $\beta = 0.01$, $\beta_i = 0.8$, $\lambda_1 = 0.2$, $Q = 4$, $\phi = 0.6$, $x = 0.1$, $M = 3.5$, $y = 0.4$, $K^* = 0.1$

Figure 6 has been drawn for various values of Hall parameter β_e. It can be observed from the figure that near the walls the velocity field decreases as hall parameter β_e increases, while in the middle of the channel the velocity increases. It reveals from Figure 7 that for small values of Ion-slip parameter β_i the velocity decreases but the velocity is increasing when β_i increases.

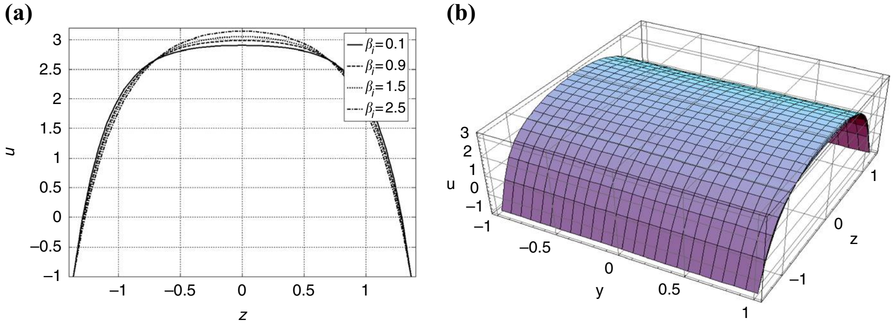

Notes: (a) For two-dimensional; (b) for three-dimensional

Figure 7. Velocity profile for different values of β_i for fixed $\beta = 0.01$, $\beta_e = 0.7$, $\lambda_1 = 0.01$, $Q = 5$, $\phi = 0.6$, $x = 0.1$, $M = 4$, $y = 0.4$, $K^* = 0.1$

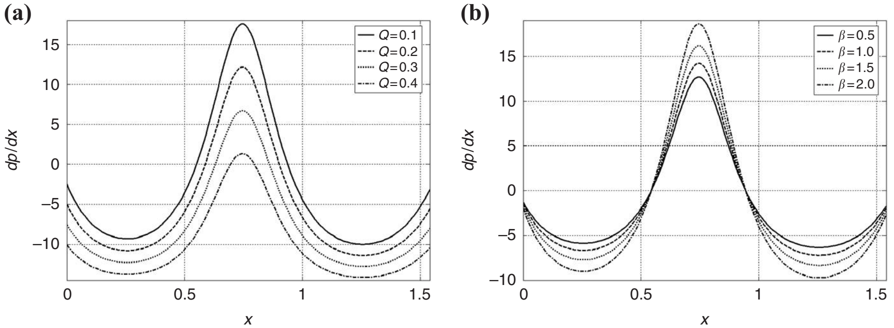

Figure 8. Variation of dp/dx (a) different values of Q; (b) for different values of β

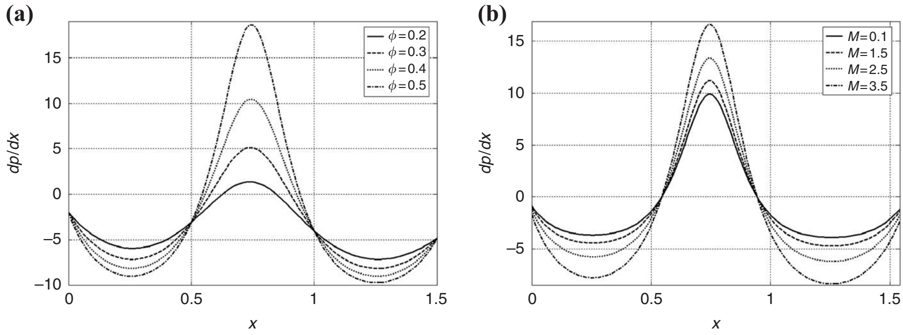

Figure 9. Variation of dp/dx (a) for different values of ϕ; (b) for different values of M

Figures 8-11 demonstrate the effects of various parameters on pressure gradient. Figure 8(a) shows the effect of flow rate Q on pressure gradient. From that fig it can be seen that pressure gradient decreases when flow rate Q increases. Figure 8(b) has been drawn for various values of aspect ratio β, it can be notice that in the wider part of the channel $x \in [0, 0.6] \in [0.9, 1.5]$, the pressure gradient is small and the flow can easily pass but in the centre of the channel when $x \in [0.61, 0.89]$, the pressure gradient is large and it increases when aspect ratio β increases. Figure 9(a) depicts that when amplitude ratio ϕ increases, the pressure gradient increases in the middle of the channel and near the walls the pressure gradient is small. Figure 9(b) describes the effects of M on pressure gradient. It is observable from the fig that for large values of Hartmann number, M the pressure gradient is decreases while in the narrow part of the channel, it increases when Hartmann number M increases. From Figure 10(a) it can be seen that the pressure gradient decreases when Jeffrey parameter λ_1 increases. It can be noticed from Figure 10(b) that when ion-slip parameter, β_i increases the pressure gradient decreases in the middle of the channel but in the wider part of the channel, his behaviour is opposite. Figure 11(a) depicts that pressure gradient is small when $x \in [0, 0.5] \in [1, 1.5]$ the flow can easily pass without any resistance of large pressure gradient, in this part the pressure gradient increases with an increases in Hall parameter, β_e, however, in the narrow part of the channel when $x \in [0.5, 1]$ a large pressure gradient is required to maintain the same flux to pass through it and in this part the pressure gradient decreases and with increase in Hall parameter β_e. Figure 11(b) presents the variation of K^* on pressure gradient, it is

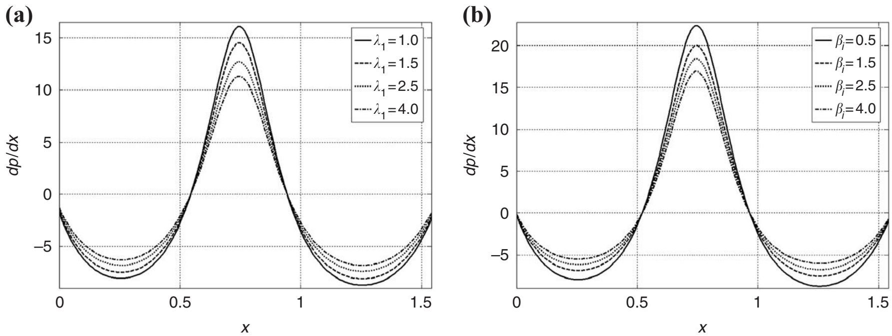

Figure 10. Variation of dp/dx (a) for different values of λ_1; (b) for different values of β_i

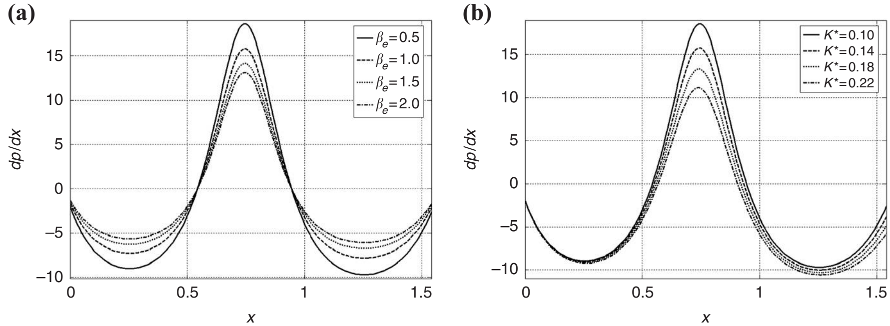

Figure 11. Variation of dp/dx (a) for different values of β_e; (b) for different values of K^*

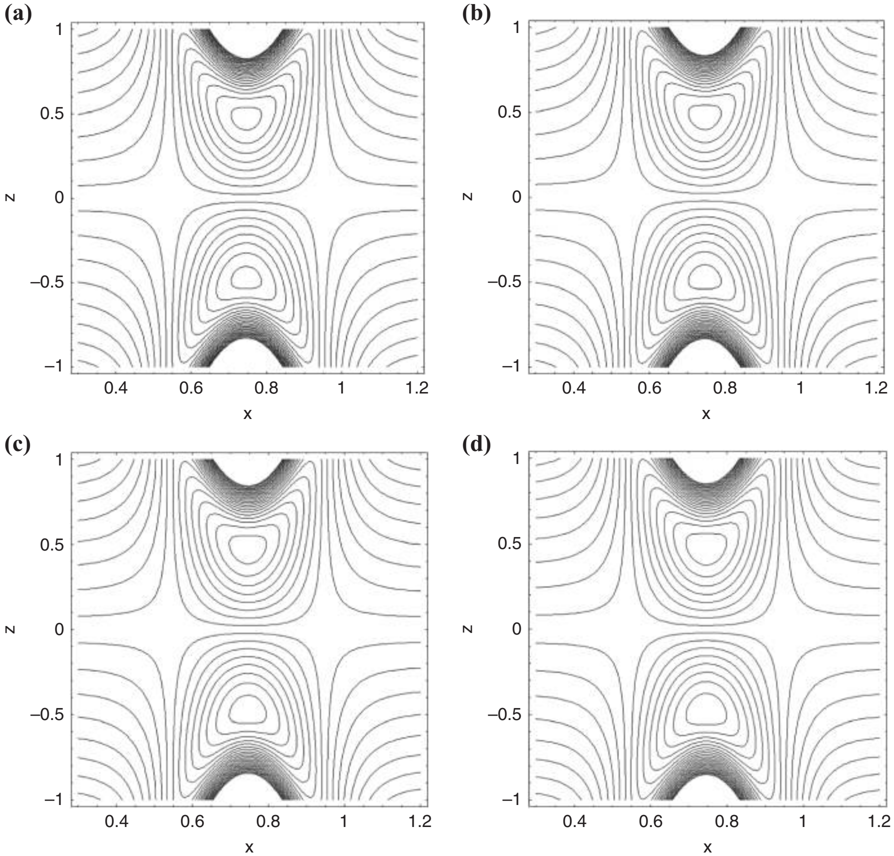

Notes: (a) For β_e=0.1; (b) for β_e=0.3; (c) for β_e=0.6; (d) for β_e=0.9. The other parameters are K^*=0.1, β=3, ϕ=0.6, β_i=0.5, M=4, λ_1=0.5, Q=0.1, y=0.4

Figure 12. Stream lines for different values of β_e

observed that pressure gradient decreases with an increase in K^*, however, it is worth mentioning that in the wider part the pressure gradient is small and the resistance is much less as compared to the centre of the channel.

4.2 Stream lines and trapping phenomena

In peristaltic motion trapping is another interesting phenomenon. Basically it is formulation of an internally circulating bolus of fluid by closed stream lines. The trapped bolus pushed a head along a peristaltic wave. In the wave frame, stream lines under certain conditions split to trap a bolus which moves as a whole with the speed of the wave. The formation of an internally circulating bolus of the fluid by closed streamline is called trapping. The bolus defined as a volume of fluid bounded by a closed stream lines in the wave frame is transported at the wave. For this purpose, the stream lines have been plotted in Figures 12-19 for various values of different parameters. Figure 12 represents the stream lines for various values of Hall parameter β_e. From this figure, it can be noticed that the with the increases of Hall parameter, β_e

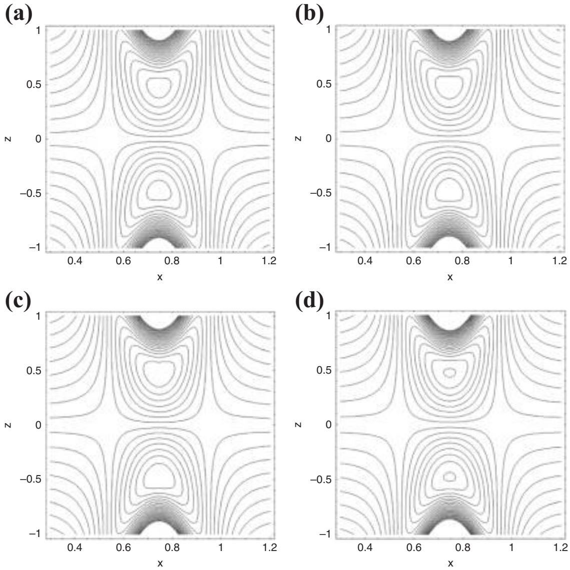

Notes: (a) For $\beta=0.5$; (b) for $\beta=1$; (c) for $\beta=1.5$; (d) for $\beta=2$. The other parameters are $K^*=0.1$, $\beta_e=0.5$, $\phi=0.6$, $\beta_i=0.8$, $M=6$, $\lambda_1=0.5$, $Q=0.1$, $y=0.4$

Figure 13.
Stream lines for different values of β

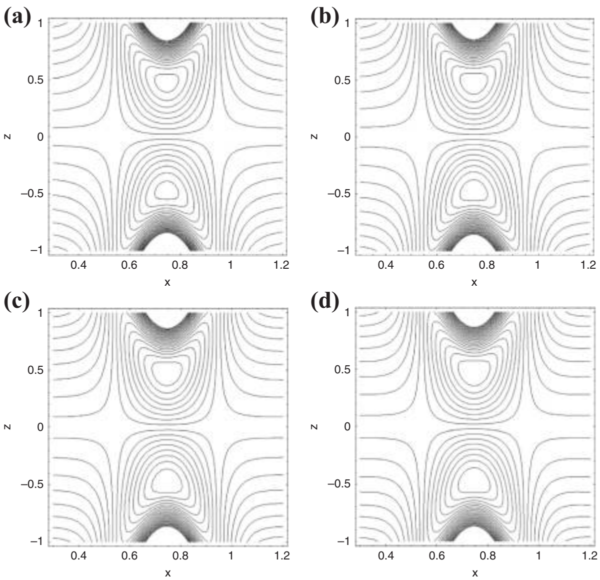

Notes: (a) For $\beta_i=0.5$; (b) for $\beta_i=2$; (c) for $\beta_i=4$; (d) for $\beta_i=6$. The other parameters are $K^*=0.1$, $\beta_e=0.5$, $\phi=0.6$, $\beta=5$, $M=9$, $\lambda_1=8$, $Q=0.01$, $y=0.4$

Figure 14.
Stream lines for different values of β_i

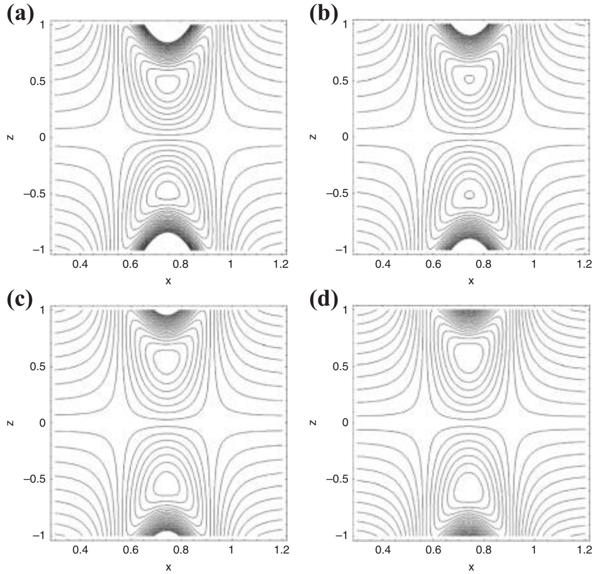

Notes: (a) For $K^*=0.1$; (b) for $K^*=0.15$; (c) for $K^*=0.2$; (d) for $K^*=0.25$. The other parameters are $\beta_i=0.1$, $\beta_e=0.9$, $\phi=0.6$, $\beta=2$, $M=5.5$, $\lambda_1=1$, $Q=0.02$, $y=0.4$

Figure 15.
Stream lines for different values of K^*

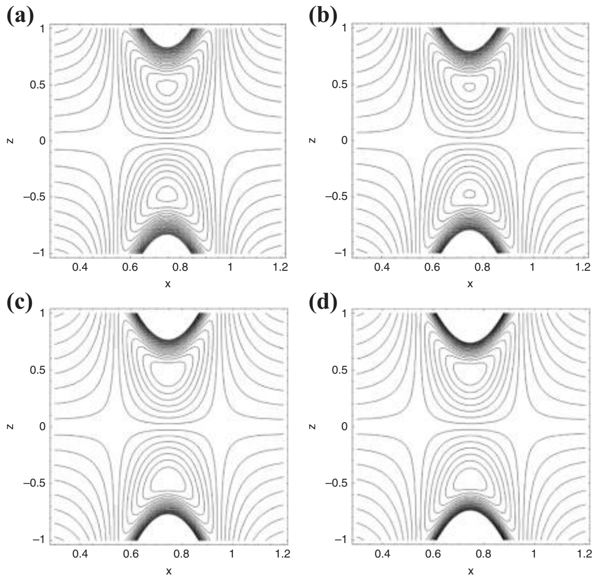

Notes: (a) For $\lambda_1=1$; (b) for $\lambda_1=3$; (c) for $\lambda_1=5$; (d) for $\lambda_1=8$. The other parameters are $\beta_i=0.95$, $\beta_e=0.8$, $\phi=0.6$, $\beta=4$, $M=6$, $K^*=0.1$, $Q=0.2$, $y=0.4$

Figure 16.
Stream lines for different values of λ_1

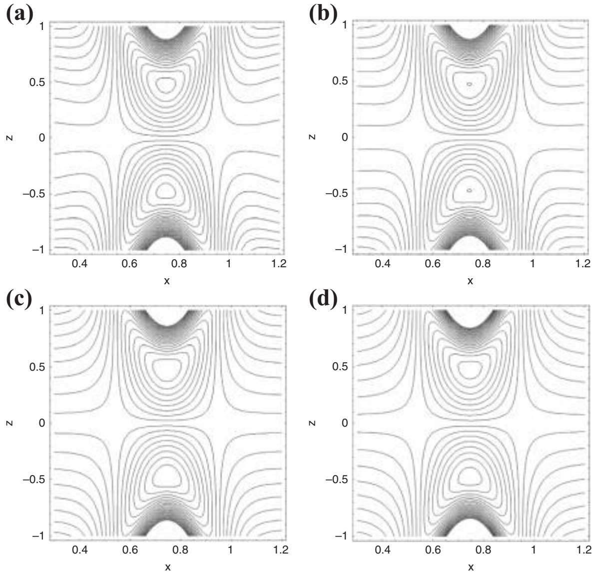

Figure 17.
Stream lines for different values of M

Notes: (a) For $M=1$; (b) for $M=2$; (c) for $M=3$; (d) for $M=4$. The other parameters are $\beta_i=0.95$, $\beta_e=0.9$, $\phi=0.6$, $\beta=2$, $\lambda_1=1$, $K^*=0.1$, $Q=0.15$, $y=0.4$

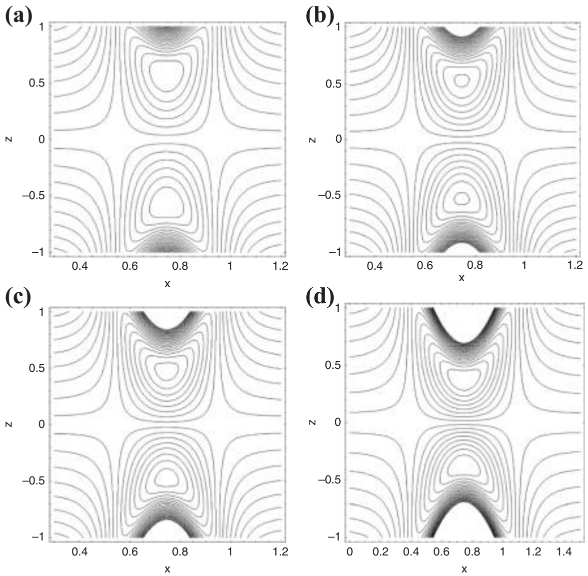

Figure 18.
Stream lines for different values of ϕ

Notes: (a) For $\phi=0.5$; (b) for $\phi=0.55$; (c) for $\phi=0.6$; (d) for $\phi=0.7$. The other parameters are $\beta_i=1$, $\beta_e=1$, $M=4$, $\beta=2$, $\lambda_1=1$, $K^*=0.1$, $Q=0.15$, $y=0.4$

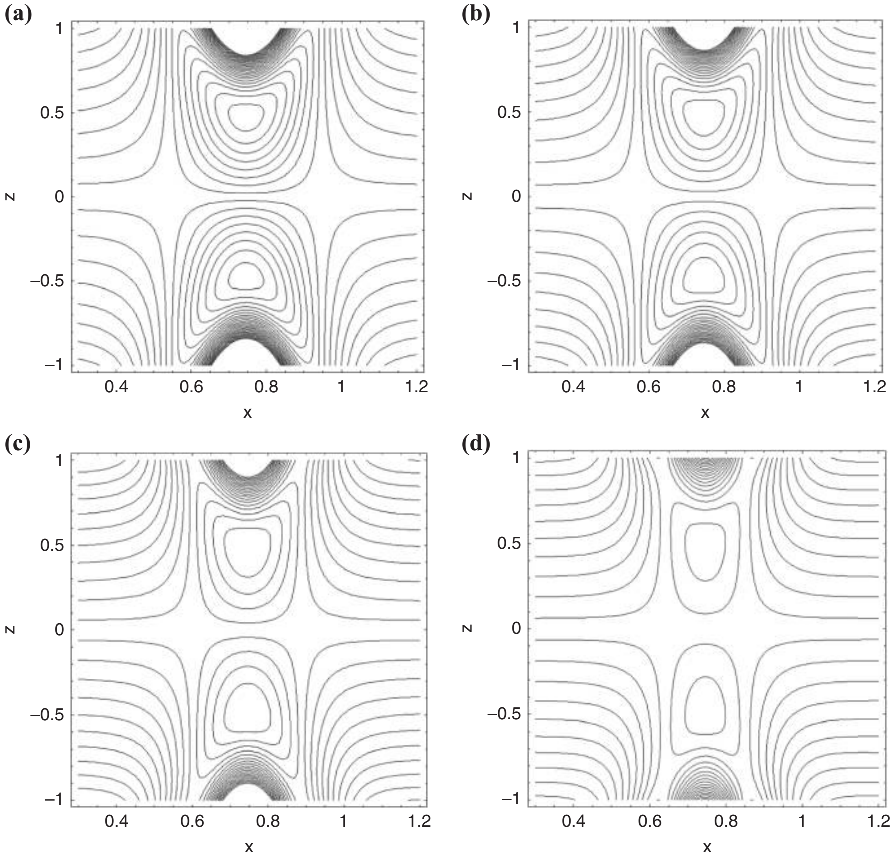

Notes: (a) For $Q=0.1$; (b) for $Q=0.2$; (c) for $Q=0.3$; (d) for $Q=0.4$. The other parameters are $\beta_i=1$, $\beta_e=0.8$, $M=0.15$, $\beta=2$, $\lambda_1=1$, $K^*=0.1$, $Q=0.15$, $y=0.4$

Figure 19. Stream lines for different values of Q

the trapping bolus increases and the size of the bolus also increases. Figure 13 depicts that when aspect ratio β increases then the size of the bolus also increases. Figure 14 describes that for large values of ion-slip parameter β_i, the trapping bolus is increasing slowly and the size of the bolus also increases. Figure 15 demonstrates that with the increase of K^* the trapping bolus reduces. From Figure 16, it can be observed that with the increase of Jeffrey parameter, λ_1 the trapping bolus reduces while the size of the bolus increases. It can be seen from Figure 17 that for large values of Hartmann number M the trapping bolus increases. Figure 18 depicts that the trapping bolus reduces when amplitude ratio ϕ increases and trapping bolus increases when ϕ decreases. Figure 19 describes that when flow rate Q increases, the size of the bolus and the trapping bolus decreases. It is noted that the MHD effects in free and augmented pumping regions are different than the peristaltic pumping region. The present analysis can serve as a model which may help in understanding the mechanism of physiological flows in channels such as such as transport of biofluids in ureters, intestines and arterioles because fluids behaves like non-Newtonian fluids.

References

Abo-Eldahab, E.M., Barakat, E.I. and Nowar, K.I. (2010a), "Effects of hall and ion-slip currents on peristaltic transport of a couple stress fluid", *International Journal of Applied Mathematics and Physics*, Vol. 2 No. 2, pp. 145-157.

Abo-Eldahab, E.M., Barakat, E.I. and Nowar, K.I. (2010b), "Hall currents and ion-slip effects on the MHD peristaltic transport", *International Journal of Applied Mathematics and Physics*, Vol. 2 No. 2, pp. 113-123.

Akbar, N.S. and Nadeem, S. (2011), "Combined effects of heat and chemical reactions on the peristaltic flow of Carreau fluid model in a diverging tube", *International Journal of Numerical Methods in Fluids*, Vol. 67 No. 12, pp. 1818-1832.

Akram, S. and Nadeem, S. (2013), "Influence of induced magnetic field and heat transfer on the peristaltic motion of a Jeffrey fluid in an asymmetric channel: closed form solutions", *Journal of Magnetism and Magnetic Materials*, Vol. 328, pp. 11-20.

Attia, H.A. (2004), "Unsteady Hartmann flow with heat transfer of a viscoelastic fluid considering the hall effect", *Canadian Journal of Physics*, Vol. 82, pp. 127-139.

Chu, W.K.-H. and Fang, J. (2000), "Peristaltic transport in a slip flow", *European Physics Journal B*, Vol. 16 No. 3, pp. 543-547.

Coleman, B.D., Markovitz, H. and Noll, W. (1996), *Viscometer Flows of Non-Newtonian Fluid*, Spring, New York, NY.

Ebaid, A. (2008), "Effects of magnetic field and wall slip conditions on the peristaltic transport of a Newtonian fluid in an asymmetric channel", *Physics Letter A*, Vol. 372 No. 24, pp. 4493-4499.

Elgazery, N.S. (2009), "The effects of chemical reaction, hall and ion-slip currents on MHD flow with temperature dependent viscosity and thermal diffusivity", *Communication in Nonlinear Science and Numerical Simulation*, Vol. 14 No. 4, pp. 1267-1283.

Ellahi, R. (2010), "Exact solutions of flows of an Oldroyd 8-constant fluid with nonlinear slip conditions", *Zeitschrift für Naturforschung A*, Vol. 65 No. A, pp. 1081-1086.

Ellahi, R. (2013), "The effects of MHD and temperature dependent viscosity on the flow of non-Newtonian nanofluid in a pipe: analytical solutions", *Applied Mathematics and Modeling*, Vol. 37 No. 3, pp. 1451-1457.

Ellahi, R., Bhatti, M.M., Fetecau, C. and Vafai, K. (2016a), "Peristaltic flow of couple stress fluid in a non-uniform rectangular duct having compliant walls", *Communications in Theoretical Physics*, Vol. 65 No. 1, pp. 66-72.

Ellahi, R., Riaz, A., Nadeem, S. and Mushtaq, M. (2013), "Series solutions of magnetohydrodynamic peristaltic flow of a Jeffrey fluid in eccentric cylinders", *Journal of Applied Mathematics & Information Sciences*, Vol. 7 No. 4, pp. 1441-1449.

Ellahi, R., Shivanian, E., Abbasbandy, S. and Hayat, T. (2016b), "Numerical study of magnetohydrodynamics generalized Couette flow of Eyring-Powell fluid with heat transfer and slip condition", *International Journal for Numerical Methods for Heat and Fluid Flow*, Vol. 26 No. 5, pp. 1433-1445.

Fetecau, C. and Fetecau, C. (2005), "On some axial Couette flows of non-Newtonian fluids", *Journal of Applied Mathematics and Physics (ZAMP)*, Vol. 56 No. 6, pp. 1098-1106.

Fetecau, C. and Fetecau, C. (2006), "Starting solutions for the motion of a second grade fluid due to longitudinal and torsional oscillations of a circular cylinder", *International Journal of Engineering Science*, Vol. 44 No. 11, pp. 788-796.

Gad, N.S. (2010), "Effect of hall currents on interaction of peristaltic flow with pulsatile magnetofluid through a porous medium", *Journal of Porous Media*, Vol. 13 No. 2, pp. 103-110.

Hameed, M. and Nadeem, S. (2007), "Unsteady MHD flow of a non-Newtonian fluid on a porous plate", *Journal of Mathematical Analysis and Applications*, Vol. 325 No. 1, pp. 724-733.

Hatzikiriakos, S.G. and Dealy, J.M. (1992), "Wall slip of molten high density polyethylene II. Capillary rheometer studies", *Journal of Rheology*, Vol. 36 No. 4, pp. 703-741.

Hayat, T., Awais, M., Asghar, S. and Hendi, A.A. (2011), "Analytic solution for the MHD rotating flow of Jeffery fluid in a channel", *ASME Journal of Fluid Engineering*, Vol. 133, pp. 0612011-0612017.

Kothandapani, M. and Srinivas, S. (2008), "Peristaltic transport of a Jeffrey fluid under the effect of magnetic field in an asymmetric channel", *International Journal of Non-Linear Mechanics*, Vol. 43 No. 9, pp. 915-924.

Lajvardi, M., Moghimi-Rad, J., Hadi, I., Gavili, A., Isfahani, T.D., Zabihi, F. and Sabbaghzadeh, J. (2010), "Experimental investigation for enhanced ferrofluid heat transfer undermagnetic field effect", *Journal of Magnetism and Magnetic Materials*, Vol. 322 No. 21, pp. 3508-3513.

Luk, S., Mutharasan, R. and Apelian, D. (1987), "Experimental observations of wall slip: tube and packed bed flow", *Industrial and Engineering Chemical Research*, Vol. 26 No. 8, pp. 1609-1616.

Makinde, O.D. and Onyejekwe, O.O. (2011), "A numerical study of MHD generalized Couette flow and heat transfer with variable viscosity and electrical conductivity", *Journal of Magnetism and Magnetic Materials*, Vol. 323 No. 22, pp. 2757-2763.

Mansour, M.A., El-Hakiem, M.A. and El Kabeir, S.M. (2000), "Heat and mass transfer in magnetohydrodynamic flow of micropolar fluid on a circular cylinder with uniform heat and mass flux", *Journal of Magnetism and Magnetic Materials*, Vol. 220 No. 2, pp. 259-270.

Mekheimer, K.S. (2003), "Non-linear peristaltic transport of magnetohydrodynamic flow in an inclined planar channel", *Arabian Journal of Science and Engineering*, Vol. 28 No. 24, pp. 183-201.

Migler, K.B., Hervet, H. and Leger, L. (1993), "Slip transition of a polymer melt under shear stress", *Physical Review Letter*, Vol. 70 No. 3, pp. 287-290.

Piau, J.M. and El Kissi, N. (1994), "Measurement and modelling of friction in polymer melts during macroscopic slip at the wall", *Journal of Non-Newtonian Fluid Mechanics*, Vol. 54, pp. 121-142.

Rajagopal, K.R. (1978), "Thermodynamics and stability of non-Newtonian fluids", PhD thesis, University of Minnesota, Minneapolis, MN.

Rajagopal, K.R. (1982), "A note on unsteady unidirectional flows of a non-Newtonian fluid", *International Journal of Non-Linear Mechanics*, Vol. 17 No. 5, pp. 369-373.

Rajagopal, K.R. (1983), "Longitudinal and torsional oscillations of a rod in a non-Newtonian fluid", *Acta Mechanica*, Vol. 49 No. 3, pp. 282-285.

Rajagopal, K.R. and Gupta, A.S. (1984), "An exact solution for the flow of a non-Newtonian fluid past an infinite plate", *Meccanica*, Vol. 19 No. 2, pp. 158-160.

Rathod, V.P. and Mahadev, M. (2012), "Peristaltic flow of Jeffrey fluid with slip effects in an inclined channel", *Journal of Chemical and Biological Physical Science*, Vol. 2 No. 4, pp. 1987-1997.

Roux, C.L.E. (1999), "Existence uniquueness of the flow of second grade fluids with slip boundary conditions", *Archives of Rational Mechanics Analysis*, Vol. 148 No. 4, pp. 309-356.

Safia, A., Ghafoor, A. and Nadeem, S. (2012), "Mixed convective heat and mass transfer on a peristaltic flow of a non-Newtonian fluid in a vertical asymmetric channel", *Heat Transfer Asian Research*, Vol. 41 No. 7, pp. 613-633.

Srinivasacharya, D. and Kaladhar, K. (2012), "Analytical solution of mixed convection flow of couple stress fluid between two circular cylinders with Hall and ion-slip effects", *Turkish Journal of Engineering and Environmental Science*, Vol. 36 No. 3, pp. 226-235.

Subba Reddy, M.V., Mishra, M., Sreenadh, S. and Rao, A.R. (2005), "Influence of lateral walls on peristaltic flow in a rectangular duct", *ASME Journal of Fluids Engineering*, Vol. 127 No. 4, pp. 824-827.

Tan, W.C. and Masuoka, T. (2005), "Stokes' first problem for a second grade fluid in a porous half space with heated boundary", *International Journal of Non-Linear Mechanics*, Vol. 40 No. 4, pp. 512-522.

Tan, W.C. and Masuoka, T. (2007), "Stability analysis of a Maxwell fluid in a porous medium heated from below", *Physics Letter A*, Vol. 360 No. 3, pp. 454-460.

Taneja, R. and Jain, N.C. (2004), "MHD flow with slip effects and temperature-dependent heat source in a viscous incompressible fluid confined between a long vertical wavy wall and a parallel flat wall", *Defence Science Journal*, Vol. 54 No. 1, pp. 21-29.

Tsangaris, S. and Vlachakis, N.W. (2003), "Exact solution of Nvier-Stokes equations for the fully developed pulsating flow in a rectangular duct with constant cross-sectional velocity", *ASME Journal of Fluids Engineering*, Vol. 125 No. 2, pp. 382-385.

Vinogradov, G.V. and Ivanova, L.I. (1968), "Wall slippage and elastic turbulence of polymers in the rubbery state", *Rheologia Acta*, Vol. 7 No. 3, pp. 243-254.

White, J.L., Han, M.H., Nakajima, N. and Brazoskowski, R. (1991), "The influence of materials of construction on biconical rotor and considerations of slippage", *Journal of Rheology*, Vol. 35 No. 1, pp. 167-189.

Further reading

Ellahi, R., Riaz, A. and Naeedm, S. (2014), "A theoretical study of Prandtl nanofluid in a rectangular duct through peristaltic transport", *Applied Nanoscience*, Vol. 4 No. 6, pp. 753-760.

Corresponding author
Ioan Pop can be contacted at: popm.ioan@yahoo.co.uk